NASA-CR-202576

Annual Performance Report
for the period 1 January 1996 - 31 December 1996

for

NASA Grant No. NAGW-4250

entitled

REMOTELY SENSED INDEX OF DEFORESTATION/URBANIZATION FOR USE IN CLIMATE MODELS

submitted to

Ms. Ming Ying Wei
Technical Officer
NASA Headquarters
Code YS
300 East Street SW
Washington DC 20546

by

Toby N. Carlson
Principal Investigator
Department of Meteorology

The Pennsylvania State University
Office of Sponsored Programs
110 Technology Center
University Park PA 16802

November 19, 1996

1. Introduction

We have completed an investigation of urbanization in the State College area and have begun work on two additional target sites: Chester Co., Pennsylvania, and Costa Rica. State College served as a test area for developing our methodology: the target area is small and lightly populated, but it is undergoing rapid urbanization. Chester Co., however, is much larger, and is riddled with urban centers, some of which are undergoing rapid development, --mostly at the expense of farmland; (*ref.*, Table 2, Section 2). Costa Rica is undergoing both a very high rate of urbanization around its principal city, San Jose', and had been experiencing a very large overall rate of deforestation (about 4% a year) until a decline began a few years ago.

The purpose of the investigation is to use a new method for deriving land surface parameters from a combination of thermal infrared and vegetation index measurements obtained by satellite (Landsat-TM and NOAA-AVHRR) and to integrate these parameters with more conventional data bases. Our intent is to show that it is possible not only to monitor land use changes over time by satellite with conventional descriptors (percent developed, agriculture, forest, water) but to express these same land use change in terms of physically based surface climate variables derived from the satellite measurements, -- moisture availability (Mo) and fractional vegetation cover (Fr). By physically based we mean that the surface energy fluxes can be calculated from these two parameters, which are the dominant ones governing the surface energy budget in land surface models. Moreover, given a field of Mo and Fr and a specific urbanization or deforestation scenario, future changes in local microclimate can be made with the aid of a atmospheric mesoscale model.

Underlying all this work is our basic hypothesis, which is that changes in land use, including deforestation, exert a profound influence on local microclimate whose effects may greatly exceed in importance those occurring on larger scales. We hope to establish for the first time a systematic and quantitative approach to classification of images using

thermal infrared (and vegetation index) measurements by satellite, from which the urban planner, the meteorologist and the geographer can assess both past and future impact on the environment.

2. Present Investigation

a) A Review of Results from the State College study

A major research effort in our research has been devoted to the study of urbanization using the so-called triangle method (Gillies and Carlson, 1995; Gillies et al., 1997). In the first phase, Owen (1995; see also Owen *et al.*, 1996 and Carlson and Owen, 1996 (attached)) completed an analysis of the State College, PA, area in which values of Fr and surface moisture availability, Mo,. were determined from AVHRR data over a 30x30 km domain centered on State College, PA. The object was to see if the migration of pixels within the Fr/Mo space (the triangle) were coherent and could be related to the nature and extent of urbanization. Eight AVHRR scenes were obtained (two per summer every other year) between 1986 and 1994. Additional Landsat TM scenes were obtained, from which percent urban development was calculated and classified as to forest, agriculture, developed and water.

Results, summarized in Owen *et al.* (1996) and Carlson and Owen (1996), are that (1) AVHRR data can detect neighborhood-scale changes in urbanization, (2) moisture availability (Mo) seems to constitute an intrinsic descriptor of the surface fabric, in addition to being a fundamental land surface parameter which governs local microclimate, (3) changes in Fr and a scaled infrared surface radiant temperature (T^*_r) (as well as evapotranspiration) accompany significant changes in urbanization; Mo, however, does not appear to change significantly with increasing urbanization, at least when agricultural land is developed; Fr decreased substantially from the summer of 1985 to the notoriously dry summer of 1988 (but recovered in 1991), whereas Mo hardly changed during that

period. (4) tree cover appears to be a dominant mitigating factor in the aforementioned changes in land surface parameters. Tree cover seems to affect Mo.

b) Chester Co.

Following our methods developed for State College, analyses have begun of images for Chester County, PA. Chester Co., located just west of Philadelphia, is about four times the area of the State College target area. Parts of the county are undergoing rapid urbanization.

Table 1: List of Scenes Obtained for Chester Co.
(AVHRR and Landsat Thematic Mapper)

AVHRR	Landsat - TM
7/24/85	6/10/87
7/5/86	7/12/87
7/16/88	6/12/88
7/12/89	5/20/91
8/2/90	7/28/93
9/1/90	6/2/96
7/10/91	
8/17/91	
8/22/92	
7/17/93	
8/24/94	
7/15/95	
7/16/95	

AVHRR scenes from 1986 to 1995 (Table 1) have been converted to temperature and radiance values, corrected for atmospheric attenuation and georeferenced; this has also

been done for a fewer number of Landsat TM scenes covering roughly the same period. Initially, the procedures parallel those applied to the State College images. As in the case of State College, summer scenes are used because they are subject to the least variability due to changing meteorological conditions, and because summer scenes permit a better distinction between forest, agriculture and developed land than spring or winter scenes. From these image data, we determine Mo and Fr and then relate these parameters to the conventional land use categories as they evolve over the previous decade.

All TM images have been classified according to several basic land surface types. Although the latter operation involves designating a variety of different land surface types, the final analysis consolidates all classes into four categories: -- developed, forest, agriculture (including pasture and bare land) and water. A summary of these four classes by percent is listed below in Table 2. The table shows a progressive increase in developed land, which occurred largely at the expense of farmland. Unlike the corresponding values for State College, forested area in Chester Co. underwent a small but non-trivial decline. Much of this decrease in forested area pertains to the loss of trees in and around new developments, rather than the loss of land formally designated as forest. Instead, new housing in wooded areas in at least partly responsible for the decline in the forest category.

Table 2: Percentage Classified for Each Category, Chester Co.

Sfc. Type	1987	1988	1991	1993	1996
Agriculture	71.8	70.8	69.3	67.5	66.0
Forest	16.8	16.9	15.1	14.7	14.7
Developed	10.9	11.6	15.1	16.3	19.0
Water	0.5	0.6	0.45	0.38	0.3
Cloud, etc.	0.01	0.15	0.0	1.02	0.0

Validation

To verify these statistics, several approaches have been taken. The first was to compare our designated categories with those determined by aircraft and in situ methods, as published by the Chester Co. planning office in West Chester, PA (courtesy of Mr. Wayne Clapp), with whom we have maintained a cordial relationship. The published classification for 1987 was compared with our 1987 classification based on the Landsat image. We then determined a verification matrix from which we calculated user accuracy and producer accuracy (Congalton, 1991). These results are shown in Table 3.

Table 3. User and Producer Accuracy: Chester Co. (1987 Survey)

Sfc. Type	User Accuracy	Producer Accuracy
veg/crops	76	96
forest	87	75
developed	93	54
water	100	100

User accuracy is calculated by dividing the number of correctly classified pixels in a land cover category by the total number of pixels classified in that particular category. This statistic represents the probability that a pixel classified using remotely sensed data actually represents that class. The producer's accuracy is calculated by dividing the number of correctly classified pixels in a land cover category by the total sum of that category. This represents the probability that a reference pixel is correctly classified. For example, the producer of the 1987 classified image can claim only that 54% of the time an area that was actually developed was identified as such. However, a user of the

classification map will find that if they were to visit a site that the map indicates is developed, 93% of the time it will have been developed.

A second method, which is based on determining the so-called the KHAT statistic (Congalton, 1991),involves not only the correctly classified pixels but the off-diagonal elements in the matrix. KHAT takes into consideration confusion among classes. For the 1987 image, the result is a KHAT of 81%, which implies that the classification process avoided about 4/5 of the errors that a completely random classification would generate. This result is in agreement with other remotely derived land cover classifications (Tin-Seong, 1995).

Producer accuracy tends to be lower for developed areas than non-developed areas because of confusion between medium density buildings and bare soil; Tin-Seong (1995) found that this ambiguity accounted for about one-third of the error. In our 1987 image, developed areas were predominantly misclassified as either vegetated grassy field or forests. Spectral confusion of land cover types is aggravated by the spatial heterogeneity and mixed pixels typical of urban settings. Developed areas tend to include a considerable interpixel and intrapixel variation which is found less over forests or water bodies. Above all, a distinction must be made between spectral and societal classifications. Both may be correct within their own context.

Additional significance testing for the Landsat classification when combined in 1 km squares (*ref.* discussion below) in order to assess the confidence in determining the percentage of developed area. Classified Landsat TM images were subset into 1 km squares (roughly comparable to the resolution of the AVHRR), each containing 1600 pixels assigned to one of the five categories listed in Table 2. From this arrangement, a 2x2 matrix was created for each of the 1 km pixels for two images at two different years; this is shown below in Table 4.

The diagonal elements represent pixels which have experienced no change in classification between the two times in question. Off-diagonal elements represent pixels which have changed from either undeveloped to developed or vice versa. A null hypothesis of no change over time is equivalent to a hypothesis of symmetry in the matrix. No development in time requires that the off-diagonals must be either zero or that $X_{12} = X_{21}$, which is to say that as many pixels changed from undeveloped to developed as from developed to undeveloped.

Table 4. Matrix for obtaining p-value for development assessment

Time 1	Time 2	
	Developed	Not Developed
Developed	X_{11}	X_{12}
Not Developed	X_{21}	X_{22}

Following Eliasziw's (1991) McNemar test for a 2x2 table, we are testing the null hypothesis of marginal symmetry by calculating the p-value: $(p(\chi_1^2 \geq z^2)$, where

$$z^2 = \frac{(X_{12} - X_{21})^2}{(x_{12} + x_{21})}$$

The p-value is determined by comparing the z^2 value to a chi-square distribution density function with one degree of freedom, which yields the probability of obtaining a $\chi 2$ greater than or equal to the calculated z^2 value. A low probability indicates strong evidence that the off-diagonals are not symmetric and there has been a significant change in land use over time.

Qualitatively, at least, the general development trend demonstrated by Landsat TM classified images reflect the changes which have been reported for Chester Co. by the Chester Co. Planning Commission. These patterns of change, shown by the classified TM images for 1987 and 1996 (Figures 1a and b) reflect continued suburban expansion outward from Philadelphia (denoted by the letter 'a' in Figures 1a and b) into eastern Chester Co., as well as the development of 'bedroom communities' out of Delaware

June 10, 1987

Land Cover Classification

Chester County, PA and Surrounding Area

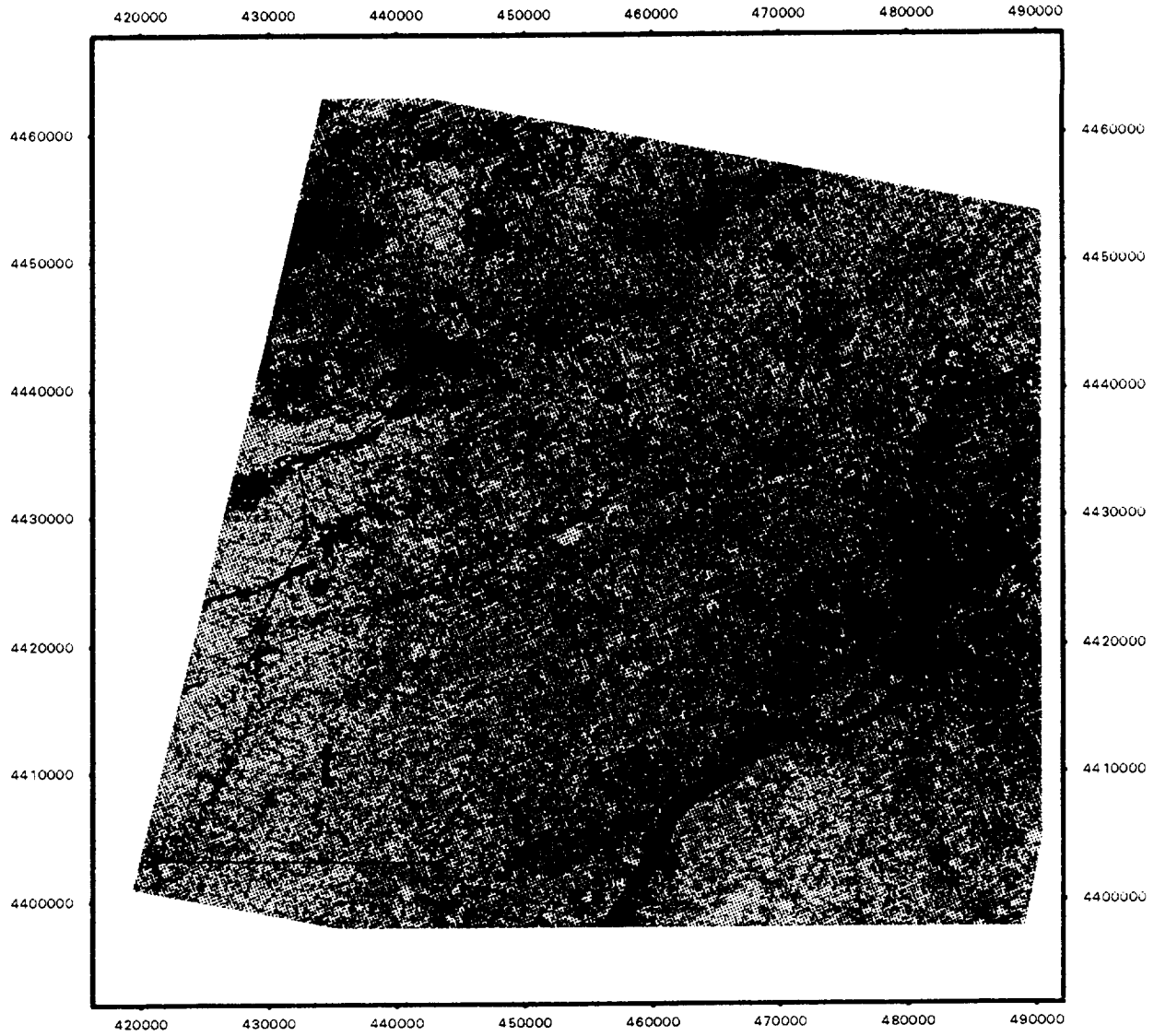

Legend

- bare soil 1
- bare soil 2
- partially vegetated
- scrubby vegetation
- vegetated / grassy field
- forest
- water
- developed
- cloud cover

Scale

20 0 Kilometers

10 0 Miles

N

derived from Landsat TM imagery
georeferenced to UTM map coordinates, Zone 18

Figure 1a. Classified Landsat TM image for June 10, 1987 over Chester Co. Letters denote locations referred to in the text. The outline of Chester Co. is shown by a thin solid border in the background. Categories referred to in the text (Tables 2 and 3) correspond to those in the legend except that the agricultural classification includes the five bare soil and vegetation classes.

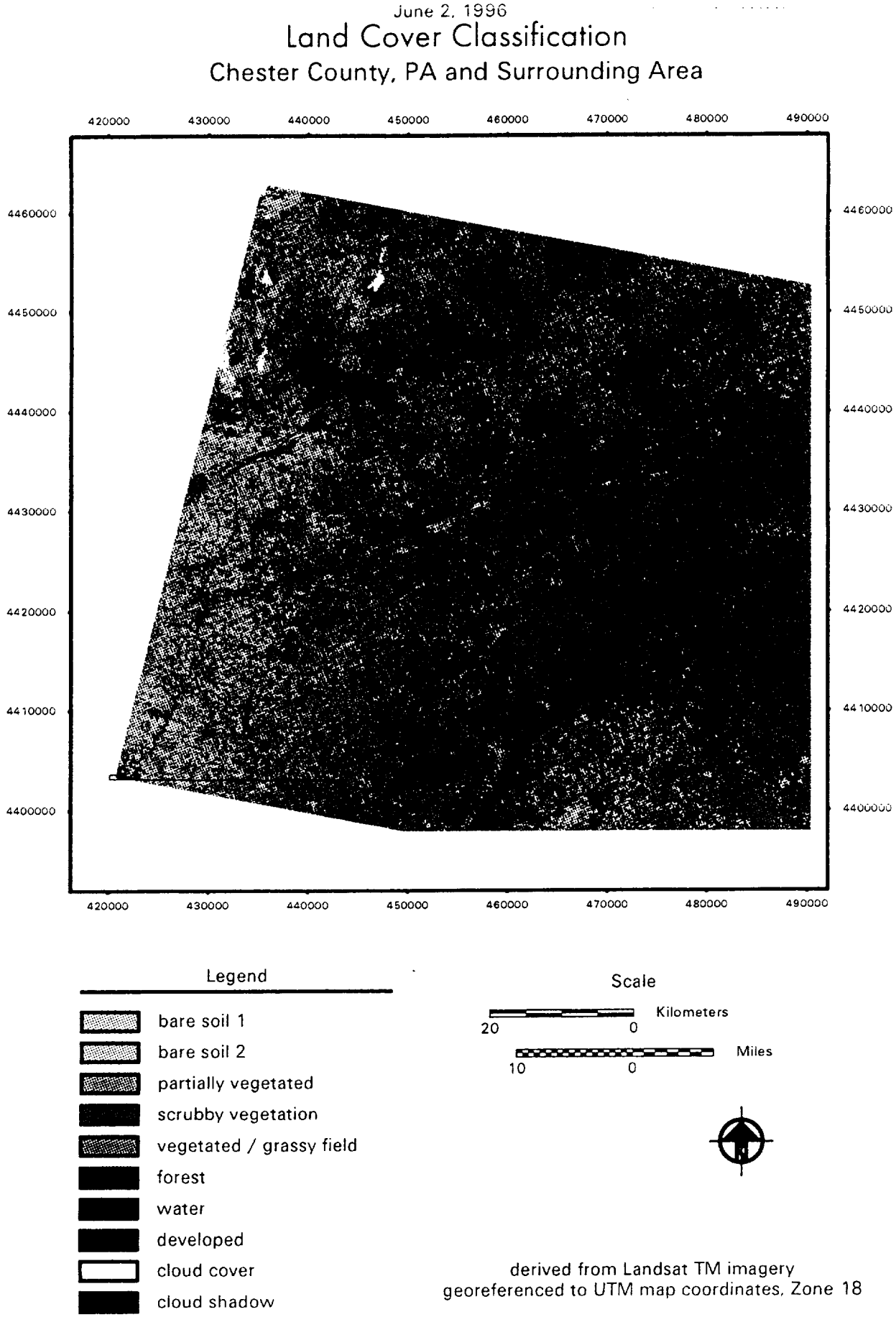

Figure 1b. Same as Figure 1a except for 2 June 1996.

(location 'e' in Figures 1a and b). At a first glance, we are likewise finding the most development between 1987 and 1996 in the West Chester borough and the surrounding townships along route US 202 in the east and along US 30 which runs through the middle of Chester Valley (location 's' in Figures 1a and b).

Present development, as revealed by Landsat, presage the Planning Commission's projected development trends for the year 2000, in which the eastern part of the county along US 30 becomes densely development and the previously distinct centers of development become more of a continuous mass stretching through the eastern half of the county. Although major roads serve as conduits for rapid and dense urbanization, many tiny, isolated pockets of development are already starting to form in the highly rural southwestern part of the county (location 't' in Figures 1a and b). These areas are projected to increase in size and number.

The decrease in forest from 1987to 1993 reflects this development pattern, as most of the land use change occurred along the US 30-202 axes. In the classification, the highly wooded residential areas of this region often appear as grids of forest and developed classes. With continual expansion of the urban fringe out of Philadelphia, the developed class expanded significantly in 1996, resulting in a loss of forest class. No loss in forest was detected between 1993 and the present.

We have also attempted to compare the 1996 classification with in situ observations made in the field. In September, we conducted a field survey of Chester Co. during which time we were able to locate (using a Trimble™ GPS meter) about 45 pixels in the Landsat image and to classify the locations visually. These statistics are currently being processed.

AVHRR images

AVHRR imagery is now being resampled and superimposed on the 1 km squares used to create the z^2 statistics referred to in Table 4. Preliminary results tend to support those of

Owen and Carlson (1997) which show that (1) neighborhood scale changes, referred to above, can be detected by AVHRR when changes in developed area is greater than 10%; (2) vegetation, notably tree cover, affects Mo more than individual precipitation events or protracted dry or wet periods; Mo appears to be an intrinsic descriptor of land surface; (3) Mo responded very little to changes in development for a given type of development; (4) fractional vegetation cover and scaled surface radiant temperature changed significantly in response to urbanization; (5) evapotranspiration decreases at approximately the same rate as the increase in developed surface area.

At present, Chester Co. images are begin transformed to values of Mo, Fr and evapotranspiration and their values at fixed UTM locations will be charted at selected locations over the past 10 years. As in the accompanying paper by Carlson and Owen (1996), pixel migrations will be followed within the context of the triangle. We plan to obtain additional land use and other socio-economic data from the Chester Co. planning office. Scatterplots and analyses of Mo, Fr and evapotranspiration should be finished by early 1997.

An example of the land use classification is shown in Figures 1a and 1b.

Costa Rica

An allied project involving deforestation in Costa Rica. Deforestation has been considerable in this country during the past 30 years. Initially, our approach will follow procedures developed for Chester Co. Unlike Chester Co and State College, land use changes have come largely at the expense of forest land, rather than agriculture. A new and vital element in our Costa Rican program is a collaboration with Professor Arturo Sanchez (currently at the University of Costa Rica), who has acquired and georeferenced a number of Landsat TM images. Professor Sanchez brings to the project a considerable knowledge of the forest resources, ecology, hydrology and demographics of Costa Rica,

as well as his expertise in image processing and analysis. He has already prepared several extensive data bases for Costa Rica.

To this data set provided by Dr. Sanchez, we have added 5 more Landsat images and six AVHRR images over a 10 year period, 1986 - 1996. AVHRR scenes will be georeferenced to the Landsat images, which have been rectified by Dr. Sanchez. A summary of these images is presented in Table 5. A few more images for 1995 and 1996 may be collected before the end of the project.

Table 5: List of Scenes Obtained for Costa Rica;
month and year). (AVHRR and Landsat TM)

Landsat-TM	Landsat-TM	AVHRR
3/75	09/88	12/85
01/76**	02/89	12/90
03/78	12/90**	01/92
12/78	03/91	12/92
01/79	03/91	12/93
01/84	12/91	01/95
02/86**	03/92	03/96
02/86	09/92	
08/86	03/93	
01/87	03/93	
01/87	04/93**	
11/87	03/94	
12/87	03/94	
	03/96**	

** Indicate usable images for San Jose area

The study centers on the capital area, San Jose' and its surroundings, where the major effects on the forest and the countryside have occurred. Not all images are usable because of extensive cloud contamination, although all dates correspond to the dry season, which extends from December through March. Starred entries in Table 5 refer to Landsat images which are sufficiently cloud free for the analysis of the deforestation and urbanization in the target area.

Georeferencing of TM images is being performed at the University of Costa Rica by Dr. Sanchez and later this winter and at Penn State for AVHRR. The PI will make one trip to Costa Rica in January and Dr. Sanchez is expected to pay a working visit to Penn State in December. Like our Chester Co. project, analyses will be made within the context of the triangle and the results related to socio-economic and ecological changes. In regard to the latter, we will attempt to use the changes in Mo, Fr and evapotranspiration to describe how the deforestation exerts pressures on the boundaries of 'life zone' (regions of uniform ecology) in Costa Rica. This part of the project will be outlined in more detail in a later report.

3. Operational Goals

Not only does scaling allow us to compare pixel values from differing images but the effect of scaling greatly minimizes errors due to atmospheric correction, instrument drift and viewing angle and therefore reduces the importance of obtaining absolute accuracy in deriving the surface parameters. Indeed, preliminary results using radiative transfer model simulations (Carlson and Ripley, 1997) shows that scaling NDVI and surface radiant temperature yields almost identical values of fractional vegetation cover and surface moisture availability as would be obtained from radiances corrected with MODTRAN, a recent variant of LOWTRAN (Kneizys *et al.*, 1988).

This is illustrated in Figure 2, which shows scaled NDVI (N*) based on the uncorrected (at sensor; $N^{*2}(a)$) and corrected (at surface; $N^{*2}(c)$) radiances. The figure not only confirms two earlier and independent validations of a square root law between scaled NDVI and fractional vegetation cover (Choudhury et al., 1994' Gillies and Carlson, 1995), but suggests that the relationship holds equally well for uncorrected as for corrected radiances.

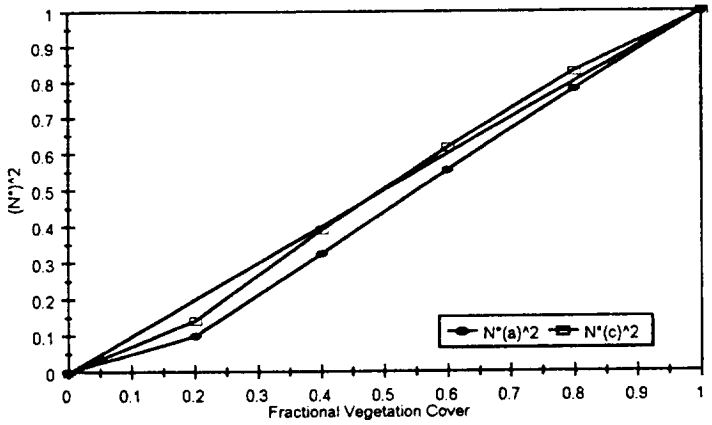

Figure 2. Simulations with a simple radiative transfer model for scaled NDVI squared (N^{*2}) versus fractional vegetation cover (Fr) based on the uncorrected (at sensor; $N^{*2}(a)$) and corrected (at surface; $N^{*2}(c)$) radiances. The solid sloping line without symbols represents a 1:1 correspondence between N^{*2} and Fr.

Scaling of temperature and NDVI not only facilitates comparison between images and scatterplots, but it greatly reduces measurement error, eliminating the need for a detailed knowledge of plant, soil or atmospheric conditions. We can also show that scaling temperature greatly reduces the atmospheric correction to the thermal radiances, just as scaling NDVI virtually eliminates the need to correct N* for atmospheric attenuation (Figure 2).

To the extent that the uncorrected and corrected NDVI values are linearly related, the atmospheric correction is eliminated from N* in scaling. Indeed, we find this to be the case (Carlson and Ripley, 1997). The result of scaling is that virtually identical values of Mo

and Fr are obtained for corrected and uncorrected values of NDVI. Errors in Mo produced by not scaling the surface radiant temperature occur because the uncorrected temperatures are not linearly related to the corrected surface temperature. In split window models, such as that of Price (1984), the atmospheric corrections depend on differences in apparent temperatures between channel 4 and channel 5 of AVHRR, and so are not necessarily linearly related to the temperature of either channel.

Consider first a scatterplot for one of the Chester images (Figure 3). Using the Price split window method we first corrected every surface temperature and then found a linear regression between the temperature corrected with MODTRAN for channel 4 of AVHRR and the apparent (uncorrected) temperature, as measured by the satellite. This established a unique correction for each value of surface temperature although the slope and intercept of the regression are based on the split window results. RMS differences between this straight line fit to the split window temperatures and the temperatures given by the split window algorithm for each pixel provide an estimate of the 'typical error' one might encounter by collapsing the split window algorithm to a simple linear regression. (The word 'error' here is simply a measure of the scatter from a straight line, as there is some question as to whether this scatter represents noise or real variations.) The RMS error in the (non-dimensional) normalized temperature (T*) for the test case (Figure 3) was ± 0.08. This value constitutes a relatively small fraction of the full range in T*, which varies from zero to one, respectively, between air temperature and the radiometric temperature of dry, bare soil.

To obtain isopleths of Mo, a polynomial relationship between Mo, N*, and T* is determined from making a range of simulations with our soil/vegetation/atmosphere/transfer (SVAT) model (Gillies and Carlson, 1995). From this output, Mo is expressed as a function of the two scaled variables; isopleths of Mo are shown in Figure 3.

From this we also compute the following expression:

$$\Delta M_o(N^*, T^*) \approx \partial M_o / \partial T^* [\Delta T^*]$$

where the partial derivative is determined by the functional form of Mo lines obtained from the simulations (the sloping lines in Figure 3) and the term in brackets on the right hand side is the RMS error referred to above. Note that this is really an estimate of the expected error in Mo based on a single case and may not precisely represent the error one would obtain in not using the split window on any other case. Further analyses of the remaining 13 AVHRR images for the Chester Co. area is being undertaken.

The implications of Figures 3 and 4 are similar to those for Figure 2 in the case of N*. The residual error in not making atmospheric corrections to surface radiant temperature is generally less than 0.2 in Mo (20% of the full range) except for the ranges of large Mo (above 0.5 - 0.8) and large Fr (above 80%). Inasmuch as most of the points in this scatterplot lie outside this range (except for densely vegetated areas) in this test case (Figure 3), the percentage of pixels suffering a significant degradation in Mo due to neglect of an atmospheric correction is quite small. Two important implications can be drawn from this result: First, scaling is a powerful tool which may permit the use of uncorrected surface radiant temperatures, at least in an operational mode, to determine Mo and Fr from satellite data. This shortcut would significantly reduce the work required for data reduction. Second, use of a split window algorithm may not yield significant improvement over a linear least squares relationship between corrected and measured surface radiant temperature.

It is our intention to make the triangle method useful to the scientific community, which is to say for use by other scientists. The methodology is currently being prepared for display on our web site. As a first step we are creating a web site (http://www.essc.psu.edu/~tnc), from which one can access instructions on how to apply the triangle method and how to access and execute the algorithms from which Mo/Fr isopleths and scatterplots can be generated.

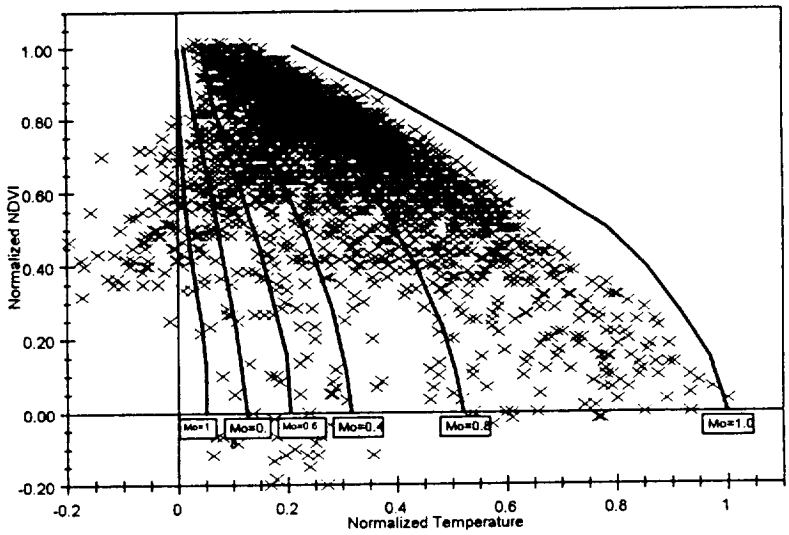

Figure 3. Scatterplot for the NOAA/AVHH image over Chester Co., 25 July, 1985. Normalized surface radiant temperature (T*) versus scaled NDVI (N*). The sloping vertical lines are isopleths of moisture availability (Mo)

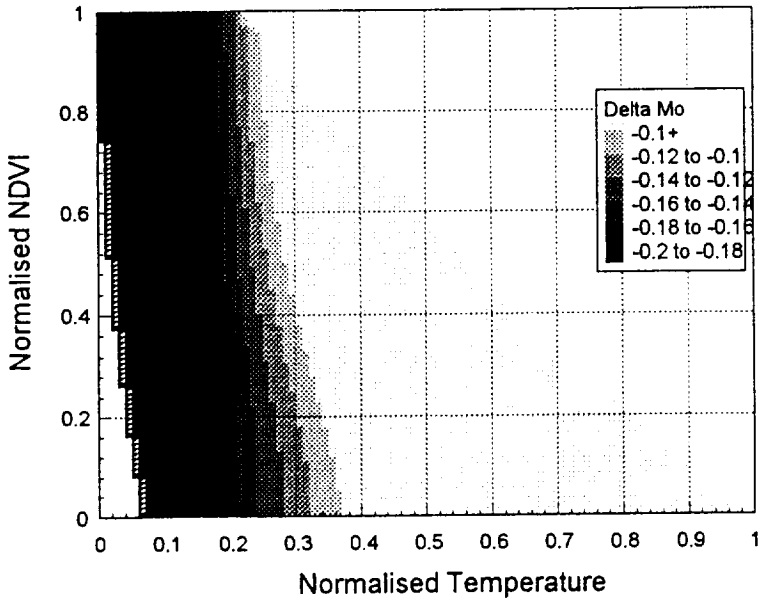

Figure 4. Normalized surface radiant temperature (T*) versus scaled NDVI (N*). The shaded area corresponds to the domain of the shaded region (the triangle) in figure 3 and the dark shaded area to the part of the triangle where the RMS 'error' in Mo (the RMS difference between Mo obtained from surface radiant temperatures corrected with a split window algorithm and those from uncorrected temperatures) exceeds 20% of the value of Mo. (Based on the NOAA/AVHH image over Chester Co., 25 July, 1985.)

4. Summary and Future Work

We intend to extend our State College analyses in new directions, tying the land use changes within the context of the triangle to socio-economic changes in the region and to possible local climate changes and changes in surface hydrology produced by urbanization. Ideally, we would like to produce a description of land use changes and urban development for Chester Co. in terms of changes in the climate parameters, Mo and Fr, and in the land use index developed by Owen and Carlson (1996). For Costa Rica, we will relate the changes in land surface parameters, Mo and Fr, to the so-called 'life zone' which represent areas of more or less uniform ecology. Although most of the rampant deforestation in Costa Rica has been checked during the past 5 years, our image library extends back to the 1970s when deforestation was among the highest in the world.

Preliminary results for Chester Co. show that urbanization can be detected throughout the county during the period 1987-1996, with an increase in percent of area developed from about 11 in 1987 to about 19% in 1996. Urbanization is exploding throughout the countryside and expanding rapidly from roads and highways.

Chester Co. analyses should be completed early in 1997; all Costa Rican scenes will be completed and scatterplots prepared by mid 1997. Although the Chester Co. work should be completed by the end of summer 1997, we are hopeful that this research will continue in some form beyond 1997. In anticipation that the Chester Co. results will prove to be very interesting, we have requested continued satellite coverage of both Chester Co. and Costa Rica from the ASTER project, beginning in 1998. Coverage requests, recently submitted to the ASTER project at NASA, are modest; they amount to two or three scenes every summer for Chester Co. and about the same number of scenes during the dry season (Dec - Feb) for Costa Rica. ASTER's 30 m surface resolution will allow it to replace Landsat for image classification, but its several thermal IR channels will also permit the use of split window corrections schemes for surface radiant temperature, if indeed these corrections are required. This is currently possible only with AVHRR.

Depending on the morning overpass time, ASTER may also replace AVHRR, whose overpass times are close to that of maximum surface temperature.

It is our hope that the triangle method can be simplified and streamlined such that it will lend itself to a routine applications. In so doing, it may be possible to use the fractional vegetation cover and moisture availability not only as key land use parameters in climate models but as unique indices of land use change which provide added descriptors of urbanization and deforestation beyond the conventional parameters already being employed by county planning boards.

Finally, we will be presenting a poster at an international meeting on remote sensing in France, (Physical Measurements & Signatures in Remote Sensing), to be held in Courchevel between 7 and 11 April, 1997. The subject of our poster is urbanization and deforestation in Chester Co. and Costa Rica, as viewed using the triangle method.

5. References

Carlson, T. N. and T. W. Owen, 1996:Monitoring urbanization and urban climate by satellite. *Proceedings for symposium on monitoring urbanization and urban climate by satellite, Human Interactions with the Environment*, Pecora13 Symposium, Sioux Falls, SD, August, 20-22, 1996.

Carlson, T. N. and D. A. J. Ripley, 1997: On the Relationship between NDVI, Fractional Vegetation Cover and Leaf Area Index. (To be submitted to Rem. Sens. Environ.)

Choudhury, B. J., N. U. Ahmed, S. B. Idso, R. J. Reginato and C. S. T. Daughtry, 1994: Relations between evaporation coefficients and vegetation indices studied by model simulations. *Remote Sens. Environ.*, **50**, 1-17.

Eliasziw, M., 1991: Application of the McNemar test to non-independent matched pair data.. *Statistics in Medicine*, 10, (Issue 12), p.1981.

Gillies, R .R. and T. N. Carlson, 1995: Thermal remote sensing of surface soil water content with partial vegetation cover for incorporation into climate models, *J. Appl. Meteor.* **34**, 745-756.
Congalton, R. G., 1991: A review of assessing the accuracy of classifications of remotely sensed data, *Rem. Sens. Environ.*, **37**, 35-46.

Kneizys, F. X., E. P. Shettle, L. W. Abreu, J. H. Chetwynd, G. P. Anderson, W. O. Gallery, J. E. Selby, S. A. Clough, 1988: *Users Guide to Lowtran-7*, Air Force Geophysics Laboratory Research Paper 401010, Project 7670, 34 pp.

Owen, T. W., T. N. Carlson and R. R. Gillies, 1996: As assessment of satellite remotely sensed land cover parameters in quantitatively describing the climate effect of urbanization, (Submitted to Int. J. Remote Sensing.)

Price, J. C., 1984: Land surface temperature measurements from the split window channels of NOAA-7/AVHRR. *J. Geophys. Res.*, **100**, 81-92.

Tin-Seong, K. A. M., 1995: Integrating GIS and remote sensing techniques for urban land cover and land use analysis. *Geocarto. International*, **10**, 39-48.

MONITORING URBANIZATION AND URBAN CLIMATE BY SATELLITE

Toby N. Carlson Professor, Dept. of Meteorology, The Pennsylvania State University, University Park, PA, 16802, USA and Timothy W. Owen Physical Scientist NOAA/NCDC, Asheville, NC, 28801., USA.

PURPOSE:

Urbanization -- the creation of industrial, commercial and residential spaces from agricultural or forested land -- has attracted the attention of climatologists since the early part of this century when the urban heat island came to be well documented. Although much has been written about the impact of urbanization on surface energy budgets and on surface air and radiant ground temperature, difficulties remain in translating this information into practical applications. We see this problems in three parts: (1) the need to translate changes in urban land use into fundamental state parameters (other than temperature) which could be used, given a particular land use change, to both describe and predict the resulting changes in urban microclimate; (2) urban planners have not yet felt the need to make use of potential climate descriptors, and (3) remote sensing is not yet appreciated as a tool in monitoring neighborhood-scale land use changes over periods of years or decades. The purpose of this paper is to indirectly address these three issues by illustrating a method for analyzing the climatic impact of urbanization using satellite measurements.

1. OVERVIEW

Unrestrained growth of cities, depletion of natural resources, the disappearance of forests along with wildlife habitats are among the main concerns of humankind as the 20th century draws to a close. Much of recent urban expansion in the United States has taken place at the expense of agricultural land, but significant loss of forested areas has also accompanied the growth of outlying urban centers. Such a transformation in the land surface profoundly affects the local microclimate. However, not all such changes in microclimate are necessarily deleterious to humans, nor is urbanization always accompanied by an increase in temperature and a decrease in vegetation amount and soil moisture; the opposite may be true for desert environments.

Our ability to monitor the climatic effects of either the beneficial or deleterious effects of deforestation and urbanization is hampered by the scale of the encroachment, by the inaccessibility of many affected areas, by constraints imposed by regional political sensibilities, and by insufficient interest or insufficient funds in the scientific community. Nevertheless, urbanization is recognizable on satellite images by changes in surface radiant temperature and vegetation index, from which estimates of soil moisture, surface runoff and vegetation fraction can be made. Most of the attention in satellite remote monitoring of urbanization has been focused on the so-called 'urban heat island'. It has become increasingly clear, however, that urbanization no longer involves a simple expansion or development of a recognizable population center but, rather, the formation and expansion of many separate commercial and residential centers about a relatively stable inner region.

Relating changes in local microclimate due to urbanization to the impact it has on human activity, such as the added or reduced energy consumption in buildings, changes in the length of growing season, *etc.*, still remains an elusive goal. More important, however, than deriving a single set of parameters; is a description of the relative and ongoing changes in microclimate that occur over years or decades and the ability to predict future changes given a specific growth scenario expressed in terms of changes in derived land surface parameters.

With very few exceptions, land use classification data, as represented in Geographical Information Systems (GIS), are expressed in terms of non-physical descriptors, such as commercial, industrial, forest, or agricultural. For example, such information is the basis of detailed maps of deforestation (*e.g.*, Sader and Joyce, 1988). Furthermore, many investigations of deforestation and land use change, based on remote surface measurements of land use and vegetation cover, tend to focus on a general description of the vegetation, *i.e.*, on estimating biomass or green foliage (Tucker *et al.*, 1984; Asrar *et al.*, 1984; Goward *et al.*, 1991), or as a qualitative tool to study specific ecosystems (Hall *et al.*, 1991). Sader *et al.* (1990), in an overview of current efforts to apply remote sensing techniques to monitor tropical forests, merely states that current satellite technology is adequate for this purpose. Thermal infrared data, however, is usually not incorporated in this analysis, but is relegated to a secondary role, such as to assess the degree of cloud contamination.

These semi-quantitative methods are, of course, highly useful for a variety of purposes (sociological and ecological) but lack the physical basis which permits the assessment of changes in microclimate. Moreover, attempts to monitor deforestation over extended periods have proved elusive, and are often highly qualitative (Sader *et al.*, 1990), although Tucker *et al.* (1985) express a guarded affirmation that satellite measurements of vegetation indices reflect trends in agricultural practices.

Remote measurements of thermal infrared temperatures have been used much more widely in studies of urbanization than for deforestation. In most cases, the focus has been on the temperature perturbation known as the urban heat island (Matson, *et al.*, 1979; Goward *et al.*, 1985; Roth *et al.*, 1989). Recent investigations, however, have begun to incorporate vegetation index measurements, along with surface radiant temperature differences between urban centers and their surroundings, as a measure of urbanization (Gallo *et al.*, 1993). While such papers tend to show a relationship between the urban-rural differences in vegetation and surface radiant temperature, they provide no information on the fundamental parameters from which predictions of future surface climate changes can be made.

There is, however, no doubt that a possibility exists to estimate, with the aid of satellites, surface variables that reflect the impact of deforestation and urbanization from the microscale (microclimate) to the macroscale (regional) climate. For example, there are clear relationships between variables such as water stress and vegetation biomass as well as a number of radiance-derived indices (e.g., Nelson *et al.*, 1987; Szekielda, 1988; Pierce *et al.*, 1990; Spanner *et al.*, 1990; Cihlar *et al.*, 1991; and Hall *et al.* 1991). Nemani and Running (1989) suggest a relationship between normalized difference vegetation index (NDVI) and a canopy resistance for deriving a measure of water stress in forests; while Thunnissen and Nieuwenhuis (1990) and Jackson *et al.* (1977) discuss an empirical land surface parameter 'B' (a constant), from which one obtains daily surface evapotranspiration. Carlson *et al.* (1981) also derived two bulk land surface parameters (the thermal inertia and moisture availability) representative of the potential for evapotranspiration at the surface. Many of these relationships, however, are based on bulk parameters, *i.e.*, those which represent the combined impact of soil and vegetation.

2. PHYSICAL BASIS

Current state of the art boundary layer schemes (*e.g.*, Taconet *et al.*, 1986; Sellers *et al.*, 1986; Abramopoulos *et al.*, 1989; Dickinson *et al.*, 1991) demonstrate the importance of calculating separate energy budgets for both soil and vegetation surfaces (expressed as proportions of soil and fractional vegetation cover). This would make surface moisture availability and fractional vegetation cover fundamental parameters in determining the surface energy budget (Avissar, 1992; Koster and Suarez, 1992; Carlson *et al.*, 1994).

Carlson *et al.* (1994) define the surface moisture availability (M_o) as the ratio of extractable surface soil water content to field capacity and the fractional vegetation cover (Fr) as the fraction of the surface visibly covered by leaves. As demonstrated by Collins and Avissar (1994) and Friedl and Davis (1994), under clear sky conditions and during day-time hours, the surface evapotranspiration is largely a function of surface moisture and vegetation cover. Thus, both parameters have precise physical meaning and are the important factors in driving the surface energy budget. As we shall illustrate, they constitute a Land Cover Index (LCI) which can be used to describe urbanization and deforestation, and serve as initial boundary conditions in the land surface components of atmospheric models (Smith *et al.*, 1994). The LCI should respond to normal seasonal evolution of the vegetation canopy or, more importantly, to direct human impact on the land surface.

2.1 Some Definitions

Isopleths of the surface moisture availability in the schematic Figure 1 are derived using the triangle method, so called because the distribution of pixels in surface temperature/vegetation space tends to form a triangular envelope (Carlson *et al.*, 1994; Gillies and Carlson, 1995; Gillies *et al*,. 1996). This method uses normalized difference vegetation index (NDVI) and surface radiant temperature (T_{ir}) to obtain surface soil water content and surface energy fluxes. NDVI, which is equated with fraction vegetation cover, is defined as

$$NDVI = \frac{(\alpha_{nir} - \alpha_{vis})}{(\alpha_{nir} + \alpha_{vis})} \qquad (1)$$

where α represents reflectance and subscripts nir and vis refer to wavelengths above and below 0.7 microns. Surface moisture availability is defined in terms of the surface evaporation over bare soil, which is:

$$LeE_o = \rho Le \frac{(q_s - q_a)}{r_{atm} + r_{ss}} = \rho LeM_o \frac{(q_s(T_{ir}) - q_a)}{r_{atm}} \qquad (2)$$

where q_a is the specific humidity of the air, $q_s(T_s)$ the saturation specific humidity at the surface radiant temperature T_{ir}, Le the latent heat of vaporization and ρ the air density.

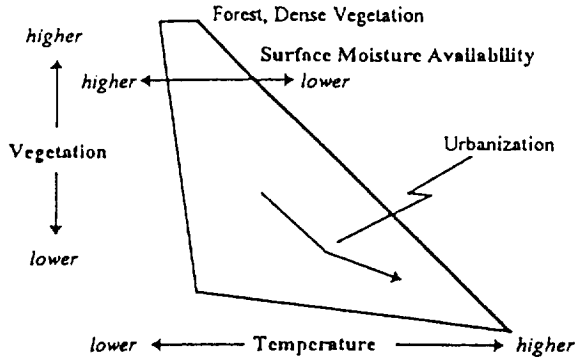

Figure 1. Schematic illustration of the triangle showing the variation of vegetation cover, surface soil moisture availability and surface radiant temperature. The darkened right border denotes the 'warm edge' and the arrow indicates a pixel migration in response to urbanization.

In order to compare scatterplots from different images, NDVI is linearly scaled between limits for bare soil ($NDVI_o$) and 100% vegetation cover ($NDVI_s$) (Choudhury *et al.* 1994; Gillies and Carlson, 1995). Scaling of NDVI is necessary when images from several days are to be compared because the absolute values of NDVI tend to vary temporally in a non-systematic manner (Price, 1987). Therefore, the scaled value is defined as

$$N^* = \frac{(NDVI - NDVI_o)}{(NDVI_s - NSVI_o)} \qquad (3)$$

Temperature is also scaled between the warmest (M_o=0; $NDVI_o$) (T_{max}) and coldest (M_o=1; $NDVI_s$) (T_s) corners of the triangle, as indicated in Figure

2; these are, respectively dry, bare soil and wet soil at 100% vegetation cover according. A scaled temperature ($\hat{T}$) is similarly defined as

$$\hat{T} = \frac{(T(Mo = 0; NDVI_o) - T_{ir})}{(T(Mo = 0; NDVI_o) - T(Mo = 1; NDVI_S))} \quad (4)$$

where $\hat{T}$ varies from zero to one as does M_o, whose isopleths extend from vertex to base of the triangle These limits are determined first by inspection of the unscaled scatterplot supplemented by simulations with a soil/vegetation/atmosphere/transfer (SVAT) model, from which isopleths of M_o and the surface energy fluxes are obtained. As the cold anchor point (M_o=1; $NDVI_s$) is consistently close to air temperature, it is customarily assigned the ambient air temperature (T_a).

An assumption in the triangle method is that M_o varies monotonically at constant NDVI from zero on the right side (the 'warm edge') to 100% of its maximum on the left side and NDVI varies monotonically with Fr. We find that the empirical relationship, $Fr \approx N^{*2}$, applies to a number of case studies (*e.g.*, Gillies *et al.*, 1996).

The importance of Fr in the surface energy balance can be seen through the following equation for the total evapotranspiration (LE_{tot}), which depends on the evaporation from bare soil (Equation 2) and transpiration from the leaves (LE_f)

$$LE_{tot} = LE_o(1 - Fr) + LE_f(Fr) \quad (5)$$

Gillies *et al.* (1996) argue that LE_f is usually close to the potential (maximum) value for a particular set of meteorological conditions unless the plant is undergoing severe water stress. As the temperature scaling (Equation 4) tends to remove fluctuations produced by changes in ambient temperature, both spatial and temporal variations in the surface fluxes and surface radiant temperature over a mix of vegetation and bare soil are strongly modulated by the fractional vegetation cover, Fr, and by M_o via Equation 2. However, the sensitivity of the latent heat flux to M_o and Fr occurs largely below about 0.4 (or 40%) (Figure 3).

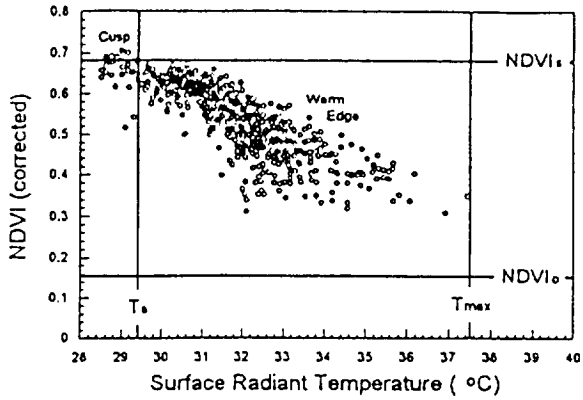

Figure 2. Scatterplot of surface radiant temperature versus NDVI over Center County, PA, for an image during June of 1994, with the warm edge labeled. Anchor values for scaling the triangle are indicated: T_a, observed air temperature, T_{max}, the temperature of bare soil and zero extractable soil water (M_o=0), bare soil ($NDVI_o$) and 100% vegetation cover ($NDVI_s$).

3. ESTIMATING M_O AND Fr: AN ILLUSTRATION

3.1 Methodology

Gillies and Carlson (1995) demonstrate that urbanization can be viewed in the context of Figure 1, in which a surface location undergoing urbanization over time will usually experience an increase in T_{ir} resulting from a reduction in both Fr and M_o. The arrow in Figure 1 illustrates this hypothesis. Relating land cover statistics with values of Fr and M_o requires the coupling of sub-pixel urban land cover data to pixel-wide values of T_{ir} and NDVI. The former was attained through the Landsat TM sensor and the latter through the National Oceanic and Atmospheric Administration (NOAA) Advanced Very High Resolution Radiometer (AVHRR).

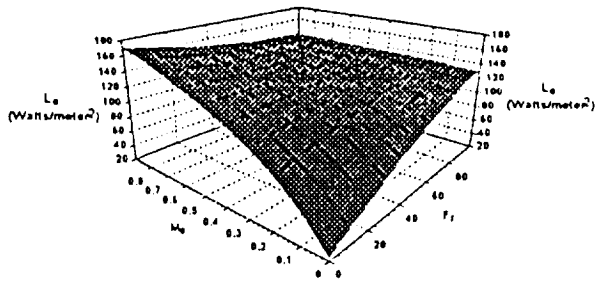

Figure 3. Sensitivity of latent heat flux LE_{tot} (Wm^{-2}) to Mo and Fr, as obtained from simulations with the SVAT model.

Figure 4 shows the location of the research study area, which encompasses a 1000 km^2 region of Centre County, Pennsylvania, USA and includes the borough of State College. This study area was selected due to its limited size, tight land-use zoning, isolation from other metropolitan areas and convenient access for field verification of the results.

With a growth rate of 9.8% during the 1980s, Centre County was a site where substantial urban development had taken place over the period in question (Centre County Planning Office, 1992). In light of this, eight AVHRR (in Level 1b format) scenes were obtained for the study area from the U.S. Geological Survey's EROS Data Center-- two single-date, Local Area Coverage (LAC) scenes each for the summers of 1985, 1988, 1991 and 1994. These scenes were selected to minimize both cloudiness and large viewing angles from nadir of the satellite; viewing angles were restricted to less than 40° to minimize unacceptable errors in reflectance values in lieu of performing a rigorous correction for angular dependency of reflectance (Paltridge and Mitchell, 1990). Given these criteria, coupled with the requirement that images be selected during the period of stable vegetation growth (from mid-June through mid-August) (Fisher, 1994), a limited number of scenes were available for selection.

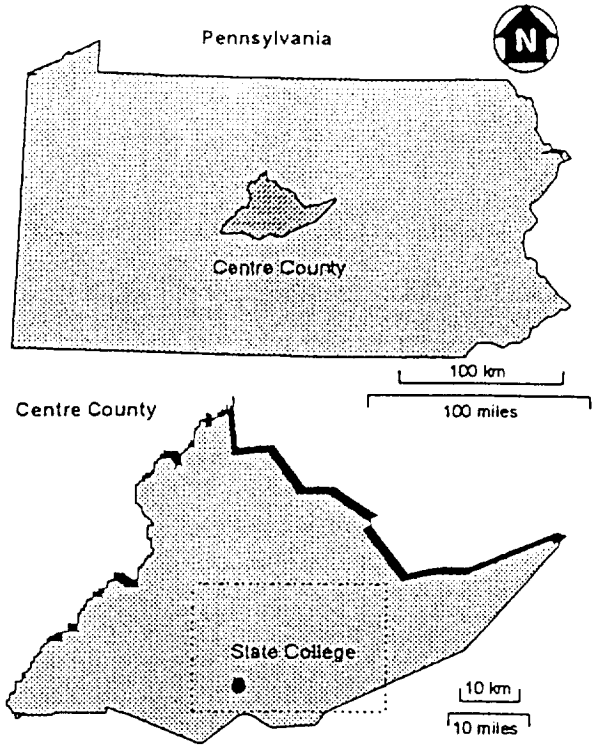

Figure 4. Location of the target area: Southern Centre CO, PA.

It was not possible, however, to completely avoid cloud and haze contaminated pixels in some scenes. Fortunately, such pixels were identified and excluded from the data analysis by using a modified cloud screening technique of Carlson *et al.* (1994). Once selected, the raw data for each of the eight AVHRR scenes was rectified and radiometrically corrected in order to assure a precise spatial and temporal inter-scene comparison (Emery *et al.*, 1989). Two Landsat TM scenes were used in this study-- one from 1986 and another from 1993. Four pairs of AVHRR images were analyzed, two for each of the summers of 1985, 1988, 1991, and 1994. Image pairs were combined into a single scatterplot for each of the four years. All AVHRR images pertain to relatively undisturbed days not immediately following significant rainfall.

A subset of each of the Landsat TM images (1986 and 1993) was taken to encompass the study area (Figure 4) and subsequently rectified (resampled to 25 meters resolution with a nearest neighbor

algorithm) to UTM (Universal Transverse Mercator) coordinates. This method of resampling was also applied to the AVHRR data as maintaining the different and discrete levels of temperature was of primary importance while in the case of the Landsat TM data set nearest neighbor resampling is considered sufficient before any form of classification is undertaken.

Radiometric correction was performed on each of the AVHRR scenes by first applying calibration coefficients provided in the ephemeris data, followed by additional algorithms. In computing surface reflectance (*i.e.*, correcting for the effects of atmospheric scattering *etc.*) value for channels 1 and 2, a bulk haze correction was applied, based upon an offset that corresponded to the minimum reflectance value for each channel (Richards, 1993). The at-sensor radiances for channels 4 and 5 were converted to at-surface-radiant temperatures.

To facilitate an accurate temporal comparison between NDVI values from all AVHRR scenes, a sensor degradation correction was applied to all NDVI values, based on the number of months between satellite launch and scene overpass (Che and Price, 1992). This corrected set of NDVI values was the final product used in the data analysis.

Land cover statistics were derived for both Landsat TM scenes (1986 and 1993). These scenes were initially subjected to a terrain normalization procedure that minimized solar illumination differences caused by topography (Hodgson and Shelley, 1994). Then, a maximum likelihood supervised level I classification of developed areas was performed according to Anderson *et al.* (1976). Five classes were distinguished-- water, forest, agriculture, developed and unclassified and ground-truthed using the following-- a 1990 EPA land cover map, Centre County aerial photographs and expert knowledge from Centre County's Planning Office (Pennick 1995, private communication). The confidence of each pixel classification was evaluated using a spectral distribution of pixel variances from the mean of each class. Those pixels that exceeded a confidence interval threshold of 95% (85% for urban) using a Chi-square statistic were reclassified as unknown. From the five known classes, land cover statistics, that included the percentage of urban development for each AVHRR pixel, were compiled from a possible 1600 Landsat TM pixels corresponding to each AVHRR pixel.

3.2 Results

Land cover was classified into three broad classes: forested, agricultural and developed. AVHRR pixel subsets for each of these classes were based upon the classified Landsat TM images. $\hat{T}$ and Fr attributes for each class were distinctly separate. The forested pixel average, for example, was centered near the point $\hat{T} = 0.17$, Fr = 0.8, while agricultural and urban pixel averages were centered at higher values of $\hat{T}$ and lower values of Fr. The separation of urban areas from other land cover types in terms of $\hat{T}$ and Fr reflects the sensitivity of vegetation and surface radiant temperature to urban land use. High spatial resolution thermal infrared measurements by Nichol (1996) suggest that such distinctions, particularly between urban and vegetated pixels, yield similar separation in the surface radiant temperature response at the resolution of a city block. Although no single pixel in the study area was completely urbanized, by implication, fully urbanized surfaces would be found where $\hat{T} > 0.9$ and Fr = 0 beyond the lower right corner of Figure 5.

From the distribution of land cover types in Fr/ $\hat{T}$ space, a land cover index (LCI) is determined. This allows the temporal process of urbanization to be quantified in terms of a location's starting point in the figure (representative of the mean influence of surrounding land cover) and the magnitude of change (representative of the urbanization process, assuming that surrounding land cover remains relatively unchanged during the time period under consideration). The spatial distribution of LCI values in the figure are determined by tangents to the one and two standard deviation ellipses normal

to an overall linear relationship between Fr and $\hat{T}$ for all eight AVHRR images. The thin curved lines are isopleths of M_o.

The LCI and M_o isopleths show the temporal relationship between the land cover parameters and urban land cover for pixels in the study area that underwent "robust development" (defined for pixels that underwent a minimum of 10% increase in development from 1986 to 1993 as defined by the two Landsat land cover classifications). Altogether 5 areas exhibited more than 10% or more urbanization, as defined in the Landsat classification; (Two of these are shown in Figure 5).

For comparison, a composite trajectory of unchanged urban pixels is shown; this was derived from the mean of an ensemble of pixels that were at least 25% developed in 1986 and underwent no further increase in development by 1993. By definition, this *control* composite pixel should remain stationary in the absence of inter-scene variability. For reasons to be discussed in the next section, the 1988 points were excluded from Figure 5.

An interesting contrast, to be discussed in the next section, is between the Park Forest (10% increase in urbanization) and the Glenview (25% increase) neighborhoods. The difference in the 1985 Fr and M_o values between the Park Forest and Glenview pixels in Figure 5 is related to the dominant surrounding land cover class for each pixel. Park Forest is predominantly deciduous forest, while the Glenview pixel consisted of formerly agricultural land with small homes, short or sparse vegetation and partially bulldozed fields. A comparison of the 1986 and 1993 Landsat classifications shows that the make-up of surrounding land cover classes in these and all five analyzed pixels remained unchanged. Thus, urban development was the primary cause of the migration of the pixels in the Fr/ $\hat{T}$ space.

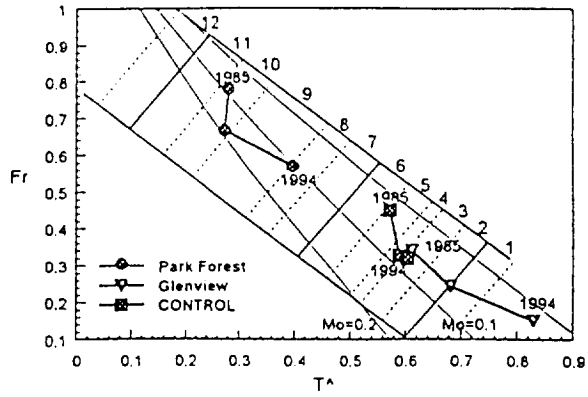

Figure 5. Temporal migrations of pixels that experienced at least 10% development between 1986 and 1993 (excluding 1988 data). The control trajectory refers to the mean values for a sample of pixels with over 25% development in 1986 that underwent no additional urbanization between 1986 and 1993.

4. DISCUSSION AND CONCLUSIONS. .

The Glenview and Park Forest trajectories, as well as those of the other three pixels (not shown) exceeding 10% urbanization, experienced similar decreases in Fr in conjunction with increases in $\hat{T}$, and similar decreases in the LCI. Surprisingly, however,. M_o exhibited little temporal variation. Although it may first appear that M_o is low at both sites, small differences in M_o may be highly important in classifying a particular site, as can be seen in Figure 3.

Another unexpected result was that the 1988 data (not shown), which corresponds to on of the warmest and driest summers on record at State College, exhibited little change in M_o from the other years. In contrast, Fr decreased notably from 1985 to 1988 to values near or below those of 1994.at all five sites. Inclusion of the 1988 data therefore gives the trajectories a more zigzag appearance, but with an unmistakable decline in Fr and increase in $\hat{T}$ at nearly constant M_o from 1986 to 1994.

Figure 6a. Photograph of Park Forest development

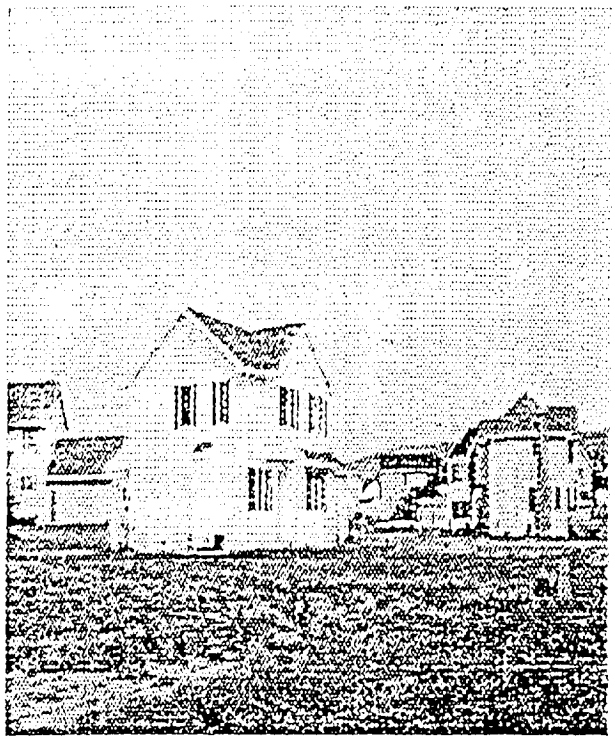

Figure 6b. Photograph of Glenview development

Differences in M_o between these Park Forest and Glenview sites are probably related to the tree cover and to the differences in the amount of bare soil visible to the radiometer. The striking contrast between Figures 6a and 6b suggests that Mo constitutes an intrinsic surface parameter independent of Fr. As Nichol (1996) has shown, bare soil can exhibit a higher radiant temperature than buildings, so that pixels closest to the warm edge may be more characteristic of undeveloped urban surfaces or unirrigated farmland than of center cities.

Finally, a significant finding is that AVHRR data can be used to classify the growth of individual housing developments. The triangle method provides a framework for examining this growth because it is relatively easy to apply and it is subject to a minimum of fluctuation due to sensor drift or changing atmospheric conditions. In portraying urbanization so graphically and in terms of parameters that govern the surface energy budget, the method may heighten awareness of the urbanization process .

The importance of trees in mitigating the climatic effects of urbanization – an idea which has begun to take hold in Atlanta, GA (Courtney, 1996; private communication) -- can not be understated. Values of LE_{tot} calculated with the SVAT model indicate that Park Forest experienced approximately a 15% decline in evapotranspiration and Glenview a 30% decline over the nine-year period with values at Park Forest being much greater than those at Glenview.

Dow and DeWalle (1995) show that urbanization produces a decline in evapotranspiration and a corresponding increase in runoff. If so, the planting of trees in urban areas would help to retain the precipitation in the ground, while not constituting an additional demand on the urban water supply. Moreover, the addition of trees in the urban setting would exert a profound impact on the local microclimate and ultimately on the power consumption both in summer (as the result of reduced air conditioning load) and in winter (due to a decreased wind loading on houses).

These effects are now indirectly quantifiable through a combination of remote sensing and mathematical modeling of land surface processes. We are currently extending this analysis to examine patterns of urbanization in Chester Co, PA, and deforestation in Costa Rica.

5. ACKNOWLEDGEMENTS

We are very much indebted to David Ripley for his assistance in image processing, calibration and correction, to Dick White, George Baumer and Doug Miller of ESSC for their advice help in acquiring Landsat images and to Phil Kolb for his help with the figures. We also received valuable information on land use statistics from Dan Pennick, the Chief Planner of Centre County. Rege Serinko of the Statistics Dept. at Purdue University was also very helpful.

We are also grateful to ESSC for their encouragement and to the National Aeronautical and Space Administration (NASA) for its financial support of this research under grant NAGW-425.
181

6. REFERENCES

Abramopoulos, F., C. Rosenzweig, and B. Choudhury, 1988: Improved ground hydrology calculations for global climate models (GCMs): soil water movement and evapotranspiration. *J. Climate*, 1, 921-941.

Anderson, J.R., E.E. Hardy, J.T. Roach and R.E. Witmer, 1976: A Land Use and Land Cover Classification System for Use with Remote Sensor Data. *U.S. Geological Survey Paper 964* (Washington, DC: USGPO, Department of the Interior

Asrar, G., M. Fuchs, E.T. Kanemasu and J.L. Hatfield, 1984: Estimating absorbed photosynthetic radiation and leaf area index from spectral reflectance in wheat. *Agron. J.*, 76, 300-306.

Avissar, R., 1992: Conceptual aspects of a statistical-dynamical approach to represent landscape subgrid-scale heterogeneities in atmospheric models. *J. Geophys. Res.*, 112, 2729--2742.

Carlson, T.N., J.K. Dodd, S.G. Benjamin, J.N. Cooper, 1981: Remote estimation of surface energy balance, moisture availability and thermal inertia. *J. Appl. Meteor.*, 20, 67-87.

Carlson, T.N., R.R. Gillies and E.M. Perry, 1994: A method to make use of thermal infrared temperature and NDVI measurements to infer soil water content and fractional vegetation cover. *Rem. Sens. Rev.*, 9, *161-173*

Carlson, T. N., R. R. Gillies and T. J. Schmugge, 1995: An interpretation of NDVI and radiant surface temperature as measures of surface soil water content and fractional vegetation cover. *Ag. and Forest Meteor.*, 77, 181-205.

Centre County Planning Office, 1992, Centre County Existing Land Use, 1990: Bellefonte, Centre County Planning Office.

Che, N. and J.C. Price, 1992: Survey of radiometric calibration results and methods for visible and near infrared channels of NOAA-7,9, and 1 AVHRRs. *Remote Sensing of Environment*, 41, 19-27.

Choudhury, B.J., N.V. Ahmed, S.B. Idso, R.J. Reginato and C.S.T. Daughtry, 1994: Relationship between evaporation coefficients and vegetation indices studied by model simulations. *Remote Sensing of Environment*, 50, 1-17.

Cihlar, J., L. St.-Laurent, and J.A. Dyer, 1991: Relation between the normalized difference vegetation index and ecological variables. *Rem. Sens. Environ.*, 35, 279-298.

Collins, D., and R. Avissar, 1994: An evaluation with the Fourier amplitude sensitivity test (FAST) of which land-surface parameters are of greatest importance for atmospheric modelling. *J. Climate*, 7, 181-203..

Courtney, R. S., 1996: Atlanta Region Commission, Atlanta, GA 30327.(Unpublished document.)

Dickinson, R.E., A. Henderson-Sellers, C. Rosenzweig, P.J. Sellers, 1991: Evapotranspiration models with canopy resistance for use in climate models, a review. *Ag. and Forest Meteor.*, 54, 373-388.

Dow, C.L. and D.R. DeWalle, 1995: Long-Term Trends in Evaporation on Urbanizing and Forested Watersheds in Pennsylvania. *Proceedings on Water Management in Urban Areas held in Houston, TX, USA on 5-9 November 1995.*

Emery, W.J., J.Brown and Z.P. Nowak, 1989: AVHRR image navigation, summary and review. *Photogrammetric Engineering and Remote Sensing*, 55, 1175-1183.

Fisher, A., 1994: Seasonal variation of vegetation indices. *Remote Sensing of Environment*, 48, 220-230.

Friedl, M. A., and F. W. Davis, 1994: Sources of variation in radiometric surface temperature over a Tallgrass prarie. *Rem. Sens. Environ.*, 48, 1-17.

Gallo, K.P., A.L. McNab, T.R. Karl, J.F. Brown, J.J. Hood and J.D. Tarpley, 1993: The use of NOAA-AVHRR data for assessment of the urban heat island. *J. Appl. Meteor.*, 32, 898-908.

Gillies, R.R. and T.N. Carlson, 1995: Thermal remote sensing of surface soil water content with partial vegetation cover for incorporation into climate models. *Journal of Applied Meteorology*, 34, 745-756.

Gillies, R.R., J. Cui, T.N. Carlson, W.P. Kustas, and K.S. Humes. 1996: Verification of the 'triangle' method for obtaining surface soil water content and energy fluxes from remote measurements of NDVI and surface radiant temperature. Submitted to *The International Journal of Remote Sensing*

Goward, S. N., C. J. Tucker, and D. G. Dye, 1985: North American vegetation patterns observed with the NOAA-7 Advanced Very High Resolution Radiometer. *Vegetation*, 64, 3-14.

Hall, F. G., D. R. Botkin, D. E. Strebel, K. D. Woods, and S. J. Goetz, 1991: Large-scale patterns of forest succession as determined by remote sensing. *Ecology*, 72, 628-639.

Hodson, M.E. and B.M. Shelly, 1994: Removing the topographic effect in remotely sensed imagery. *ERDAS Monitor*, 6, 4-6.

Jackson, R.D., R.J. Reginato, and S.B. Idso, 1977: Wheat canopy temperature a practical tool for evaluating water requirements. *Water Res. Management*, 13, 651-656.

Koster, R. D., and M. J. Suarez, 1992: Modeling the land surface boundary in climate models as a composite of independent vegetation stands. *J. Geophys. Res.*, 97, 2697--2715.

Matson, M., E.P. McClain, D. McGinnis, Jr., and J. Pritchard, 1978. Satellite detection of urban heat islands. *Mon. Wea. Rev.*, 106, 1725-1734.

Nelson, R., D. Case, N. Horning, V. Anderson, and S. Pillai, 1987: Continental land cover assessment using Landsat MSS data. *Rem. Sens. Environ.*, 21, 61-81.

Nemani, R. and S.W. Running, 1989: Testing a theoretical climate-soil-leaf area hydrological equilibrium of forests using satellite data and ecosystem simulation. *Agric. Forest. Meteor.*, 44:245-260.

Nichol, J.E., 1996: High-resolution surface temperature patterns related to urban morphology in a tropical city, a satellite-based study. *Journal of Applied Meteorology*, 35, 135-146.

Paltridge, G.W. and R.M. Mitchell, 1990: Atmospheric and viewing angle correction of vegetation indices and grassland fuel moisture content derived from NOAA/AVHRR. *Remote Sensing of Environment*, 31, 121-135.

Pennick, D., 1995: Personal communication with Chief Planner of the Centre County Regional Planning Office, Bellefonte, PA.

Pierce, L.L., S.W. Running and G.A. Riggs, 1990: Remote detection of canopy water stress in coniferous forests using the NS001 thematic mapper simulator and the thermal infrared multispectral scanner, *Photogrammetric Eng.* 56, 579-586.

Price, J.C., 1987: Calibration of satellite radiometers and the comparison of vegetation indices. *Rem. Sens. Environ.*, 21, 15-27.

Richards, J.A., 1993: *Remote Sensing Digital Analysis, An Introduction* (New York: Springer-Verlag), 340 pp.

Roth, M., T.R. Oke and W.J. Emery, 1989: Satellite-derived urban heat islands from three coastal cities and the utilization of such data in urban climatology. *Int. J. Rem. Sens.*, 10, 1699-1720.

Sader, S.A., T.A. Stone, A.T. Joyce, 1990: Remote sensing of tropical forests: an overview of research and applications using non-photographic sensors. *Photogrammetric Eng. and Rem. Sens.*, 56, 1343-1351.

Sader, S.A., and A.T. Joyce, 1988: Deforestation rates and trends in Costa Rica, 1940 to 1873. *Biotropica*, 20, 11-19.

Sellers, P. J., Y. Mintz, Y. Sud, and A. Dalcher, 1986: A simple biosphere model (SiB) for use within general circulation models. *J. Atmos. Sci.*, 6, 505-531.

Smith, C.B., M. Lakhtakia, W.J. Capehart, T.N. Carlson, 1994: Initialization of soil-water content for regional-scale atmospheric prediction models. *Bull. Am. Meteor. Soc.*, 75, 585-593.

Spanner, M.A., L.L. Pierce, S.W. Running, and D.L. Peterson, 1990: The Seasonality of AVHRR data of temperate coniferous forests: relationship with leaf area index. *Rem. Sens. Environ.*, 33, 97-112.

Szekielda, K-H., 1988: *Satellite Monitoring of the Earth.* Wiley Series in Remote Sensing, John Wiley & Sons, New York, (Jin Au Kong, ed.), 326 pp.

Taconet, O., T.N. Carlson, R. Bernard, D. Vidal-Madjar, 1986: Evaluation of a surface/vegetation model using satellite infrared surface temperatures. *J. Clim. Appl. Meteor.*, 25, 1752-1767.

Thunnisen, M., and G.J.A. Nieuwenhuis, 1990: A simplified method to estimate regional 24-h evapotranspiration from thermal infrared data. *Rem. Sens. Environ.*, 31, 211-225.

Tucker, C.J., B.N. Holben, and T.E. Goff, 1984: Intensive forest clearing in Rondonia, Brazil, as detected by satellite remote sensing. *Rem. Sens. Environ.*, 15, 255-261.

Tucker, C.J., J.R.G. Townshend, T.E. Goff, 1985: African land-cover classification using satellite data. *Science*, 227. 369-375.